Numerical Analysis of High-Power X-Band Sources, at Low Magnetic Confinement, for use in a Multi-Source Array

Philip MacInnes, Craig R. Donaldson, Colin G. Whyte, Amy J. MacLachlan, Kevin Ronald, Alan D. R. Phelps and Adrian W. Cross

***Abstract*— High-power microwave sources are typically relativistic in nature, employing multi-kilo-ampere electron beams that require significant magnetic confinement for efficient operation. As the desired output power increases so does the complexity, and overall energy requirements, of the source. It can therefore be advantageous to consider the use of several, moderate-power, sources operating as a phased array; for an array of *N* sources the far-field peak intensity scales as N^2, and the peak-of-field may be steered electronically by varying the relative phases of the different output signals. In this paper we present the numerical analysis of a short-pulse ($\sim$1ns) X-band backward-wave oscillator, driven by a 210keV, 1.4kA electron beam, suitable for use as the radiative element in such an array. Investigation of the required magnetic confinement showed two peaks in performance, with the highest efficiency, of 43%, predicted at the low magnetic confinement peak at 0.3T, corresponding to 125MW peak output power. The magnitude, and timing, of the peak in the output pulse were functions of the rise-time of the electron beam energy, with longer rise-times resulting in delayed peak-of-field and lower peak output power. When operating in an array, to maintain effective output in the region of N^2, it was determined that the beam rise-times, across all sources, should be $\leq$150ps with the adjustment of the relative timing between output's being $\pm$30ps.**

***Index Terms*— Backward-Wave Oscillators (BWOs), high power microwave generation, microwave oscillators, Slow-Wave Structures (SWSs), Phased arrays**

I. Introduction

HIGH power microwave (HPM >100MW) sources utilize high-current, relativistic, electron-beams (e-beams) to generate the electromagnetic (EM) field. For a monolithic source, as the desired output power increases so does the required electron energy, impacting on source size and complexity; manifesting in the geometry [1]–[7], and / or a move to higher mode operation [8]–[10]. This may be taken in contrast with a distributed network of (relatively) moderate-power sources, where very-high output-powers can be achieved through constructive interference of the radiated output pulses in the far-field. Operating on the same principles as the phased-array antenna, control of the temporal phase, of each source, provides both a peak radiated intensity of the order N^2, for an array of N sources, and the ability to "steer" the peak(s) of field electronically.

The Backward-Wave Oscillator (BWO) has proven suitable for use in such an array [11]–[17], where each individual BWO may be considered an independent radiative element. Efficient operation requires active control of the timing of the different outputs to ensure constructive, coherent, far-field interference, with peak operation obtained when the constituent BWOs are effectively phase-synchronous, or phase-locked. This is distinct from phase-locking of individual sources [18], [19], which refers to reduction in "jitter" of source output, though the added ability to do so is advantageous to the operation of an array; indeed, as discussed in [20], one of the methods employed to aid in phase-locking an individual source was found to greatly enhance the stability of operation in their Particle-in-Cell (PiC) simulations.

In this paper we discuss the numerical investigation of a mildly-relativistic ($\sim$200keV) BWO, designed to function at low magnetic confinement ($\sim$0.3T) as part of a dual-source array. Primarily the array size was governed by the capabilities of the intended modulator, an in-hand RADAN 303B [21], however the principle of operation applies equally to larger arrays, or maybe applied at higher power, as in [14], [22]. The intended RADAN 303B incorporates peaking and chopping spark-gaps, providing a rising edge of $\sim$100ps and a maximum pulse duration of $\sim$4ns. This places it in a region which should negate the multi-mode effects observed in [20]. Further, the source has been optimized for operation at a confining field of $\sim$0.3T, lower than used in [1], [2], [8], [14], [20], [31], providing a route to the development of lower cost, more compact, sources of HPM radiation, which again enhances suitability for use in an array.

II. Description of the BWO

The BWO is so named because it operates due to coupling of the forward-propagating Slow-Space-Charge Wave (SSCW), of the e-beam, and the backward propagating EM-wave of Slow-Wave Structure's (SWS's) operating eigenmode.

This work was supported by the European Office of Aerospace Research and Development (EOARD), of the United States Air Force Office for Scientific Research (AFOSR), under grant award FA8655-20-1-7011. The review of this article was arranged by Editor E. Choi (Philip MacInnes is the corresponding author)

The authors are with The University of Strathclyde, in Glasgow G4 0NG, UK (email: philip.macinnes@strath.ac.uk)

A schematic of a typical, azimuthally symmetric, source geometry is shown in (r,z) cross-section in Fig. 1.

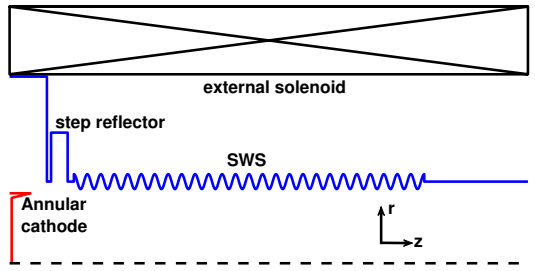

Fig. 1: Schematic of the BWO noting key components in (r,z) cross-section, - - line represents central axis.

Both the accelerating diode and interaction region are fully field-immersed using an external solenoid. This confines a thin annular e-beam, of outer radius r_b, as it is propagated close to the surface of the SWS, which is typically formed by a regular corrugation on the surface of cylindrical waveguide, in this case described as

$$r = r_0 + r_1 cos(h_z z) \tag{1}$$

where r_0 is the mean radius, r_1 is the corrugation amplitude, and $h_z = 2\pi/d_z$ where d_z is the corrugation period.

This induces periodic scattering of any propagating EM waves (discussed well in [23]), which results in the formation of eigenmodes localized within the region of the SWS. For coupling between scattered waves of the same mode these may be described as:

$$f_{w\pm} = \frac{c}{2\pi}\sqrt{(k_{z0} \pm \delta)^2 + k_c^2} \tag{2}$$

where c is the speed of light, $k_{z0} = \pi/d_z$, k_c is the cut-off wave-number of the interacting waveguide mode, and $\delta = \sqrt{\kappa^2 + k_z^2}$ is the detuning of the propagation constant k_z from k_{z0}, accounting for the strength of coupling κ between the constituent waves. For coupling between like TM modes κ may be defined as

$$\kappa = \frac{\pi r_1 k_{z0}}{2r_0} \tag{3}$$

The BWO operates in the lower TM_{01} eigenmode (f_{w-}) described by (2), with the resonant frequency (f_{res}) determined as

$$(k_z v_z - \omega_p/\gamma)^2 \approx c^2((k_{z0} - \delta)^2 + k_c^2) \tag{4}$$

where the left-hand side of (4) represents the dispersion curve of the SSCW, v_z is the axial velocity of the electron, and ω_p is the relativistic plasma frequency

$$f_p = \frac{\omega_p}{2\pi} = \sqrt{\frac{n_e e^2}{4\pi^2 \gamma m_e \epsilon_0}} \tag{5}$$

where n_e is the electron number density, e is the electron charge, γ is the Lorentz relativistic correction factor, taken as $\gamma = 1/\sqrt{(1-(v_z/c)^2)}$, or $\gamma = 1 + eV/m_e c^2$, m_e is the electron rest mass, ϵ_0 is the permittivity of free-space, and V is the applied potential.

The relation shown in (4) is approximate as it assumes an infinitely long e-beam propagating in an unbound medium. As noted in [24] the presence of the bounding drift-tube wall acts to reduce the effective plasma frequency, impacting on the intersection of the dispersion curve of the SSCW with that of the eigenmode. This has been investigated, in various forms, in [25]–[27], however a useful approximation, as made in [28] for a thin annular e-beam, is to consider the current as being uniformly distributed over the cross-section bounded by the e-beam envelope; the consequent reduction in the calculated plasma frequency, from $n_e = I/(e\pi r_b^2 v_z)$, in the authors' experience results in an intersection with the cold-dispersion of the eigenmode that is within a few percent of that predicted in PiC simulation, and measured in experiment. The curves shown in Fig. 2 arise from (2) and (4) under this approximation for parameter values inline with those used in the current study.

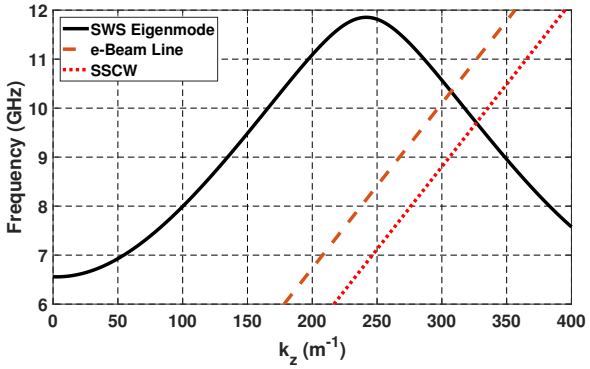

Fig. 2: Dispersion curves for SWS parameters $r_0 = 17.5$mm, $r_1 = 1.6$mm, $d_z = 13$mm, and beam parameters $V = 210$kV, $I = 1.4$kA, $r_b = 15$mm

The intersection of the SSCW and the eigenmode curves indicate the BWO would be expected to oscillate at f_{res}~9.7GHz, however the radial boundaries of the beam, the proximity of the beam to the drift-tube wall, and the strength of coupling between the SSCW and the eigenmode all impact on the exact resonant frequency. This may be understood by consideration of the field-pattern of the TM_{01} eigenmode; it will appear similar to that of the cylindrical waveguide TM_{01} mode, with a peak in the E_z field component near axis and a peak in the E_r field component near the drift-tube wall. The key difference arises in the "bending" of said E_r field component to follow the contours of the corrugation, which produces a secondary E_z peak close to the surface of the corrugation, which can then modulate a precisely located e-beam, propagating within a thin annulus. The radial location of the field-maxima in this secondary E_z peak is frequency dependent, meaning the proximity of the e-beam to the surface impacts on the frequency of modulation, albeit over a narrow bandwidth.

The step-reflector isolates the accelerating diode from the oscillations of the EM-field, redirecting the backward propagating wave towards the source output, meaning its operational

bandwidth must be at least as broad as the possible resonance bandwidth of the beam as described above. The step reflector employed here follows the work presented in [4], [29], which offers broad-band isolation, while also moving the peak-of-field away from the step transition of the drift-tube wall, reducing potential field-enhancement (improving power handling).

Beyond impacting on the resonant frequency the location, and thin annular nature of the e-beam, introduces another consideration. The beam is naturally divergent, primarily driven by the Lorentz force, arising from the imbalance in the beam's self-fields. Without additional applied magnetic insulation the annulus would rapidly expand radially and be lost to interception with the drift-tube wall. The addition of an externally applied magnetic field to mitigate this introduces the potential issue of cyclotron absorption, which occurs when the resonant frequency of the source (or its harmonics) are close to the cyclotron frequency (f_{cyc})

$$f_{cyc} = \frac{eB}{2\pi\gamma m_e} \tag{6}$$

where B is the magnetic flux density, noting that Brillouin flow, for the non-perturbed (initial) beam is [30]

$$f_p/f_{cyc} = \gamma/\sqrt{2} \tag{7}$$

In practice, the propagation of the beam, under external magnetic confinement, usually results in two peaks in the efficiency (η), where $f_{res} > f_{cyc}$, and where $2f_{res} > f_{cyc} > f_{res}$. This may be seen, for example, in [31], which shows the standard result with the higher η peak being located when $2f_{res} > f_{cyc} > f_{res}$. Post the second, higher B-field peak, η again starts to decline, then plateau, due to excessive constraint being placed on the electron motion.

III. Numerical Investigation of BWO

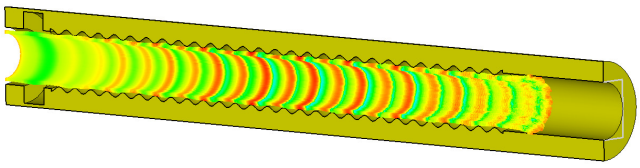

Fig. 3: Cross-section of the modeled interaction region, including particle trajectories.

The BWO interaction region, (Fig. 3), excluding the electron accelerating diode, was modeled using the PiC solver in CST: Particle Studio [32]. It consisted of a co-sinusoidal, d_z = 13mm, SWS, with the number of regular periods varied over the range 20 - 30, with tapering at either end varied over 0 - 2 periods. The mean radius was $r_0 = 17.5$mm and corrugation amplitude $r_1 = 1.6$mm. The step reflector radius was 28mm and axial length 16mm, with the separation distance (d_s) to the start of the SWS dependent on the degree of SWS tapering applied and the beam parameters used. The injected e-beam was varied in energy over the range 200keV to 250keV, with beam currents varied from 1kA to 2.5kA, and $r_b = 15$mm to 15.5mm (radial thickness at injection of 1mm). The e-beam rising-edge (t_r) was typically taken to match that of the in-hand RADAN 303B pulsed modulator at $t_r \sim$100ps rise, with a maximum e-beam duration of 4ns; this was adjustable in the simulation, separately from the runtime of the simulation as a whole.

A typical curve of the injected beam current is provided in Fig. 4, noting that the PiC model injects particles at full energy, but with current increasing to a pre-defined maximum. Also included is the corresponding temporal evolution of the number of macro-particles in simulation.

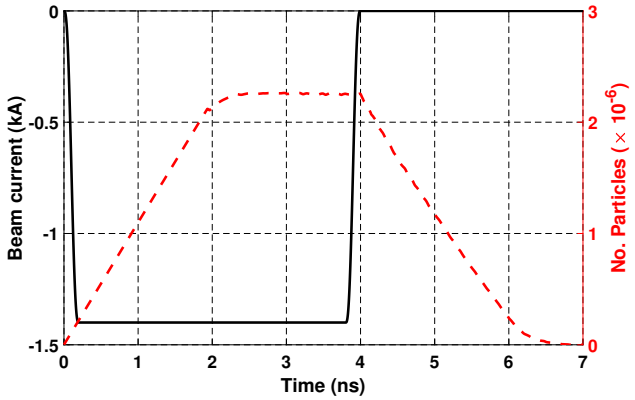

Fig. 4: Injected beam current (solid), and number of macro-particles in simulation (dashed), as functions of time.

From the current curve, the 100ps rise of the e-beam to full power may be discerned, with a corresponding fall at the termination of particle injection at 4ns. The transit time of the beam through the SWS corresponds to the first transition seen in the number of particles in simulation at $\sim$ 2ns, inline with $\sim$210keV electrons.

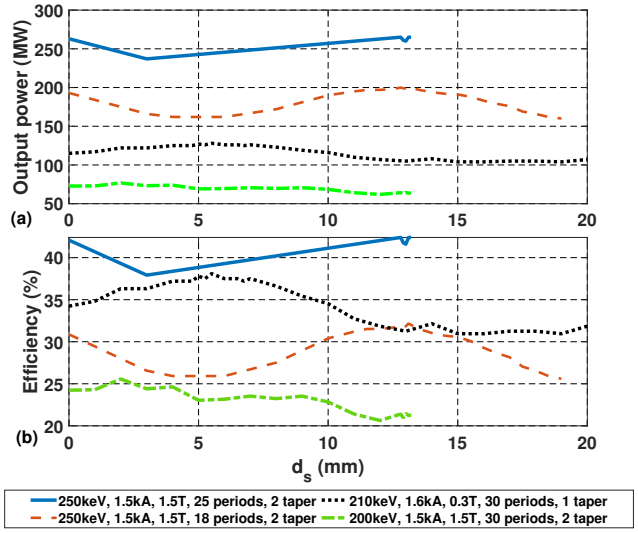

Fig. 5: (a) Output power and (b) associated η, for the BWO model as functions of the separation distance between the step reflector and the SWS (d_s), for different configurations of the interaction region. In all cases $r_b = 15$mm.

Fig. 5 shows examples of the output power, and associated

η, from a parameter study looking at different configurations of the interaction region and different e-beam parameters. This shows the expected increase in output power with increasing electron energy (Fig. 5(a)), however it also identifies a region in the parameter space where η at relatively low electron energy and B-field (210keV and 0.3T respectively) approaches that seen at higher energy and B-field (250keV and 1.5T respectively). Indeed, following further investigation and optimization of the interaction region, as shown in Fig. 6 it was observed that the low B-field, 0.3T, peak predicted higher efficiency than seen at the high B-field, 1T, peak.

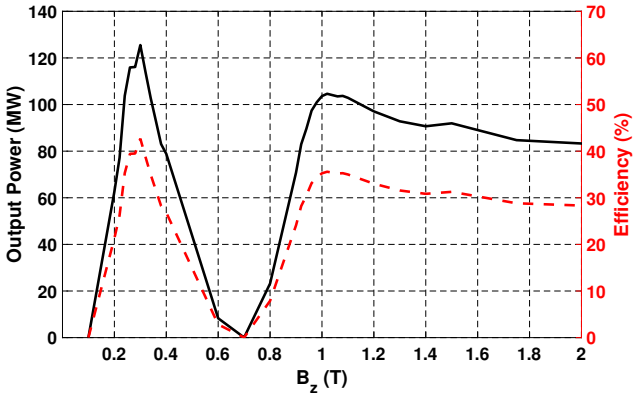

Fig. 6: Output power (solid), and associated η (dashed), as functions of the applied B-field confinement for the optimized BWO model.

The optimized interaction region consisted of a 26 period SWS, with no tapering, driven by a 210keV, 1.4kA, electron beam, rising in 100ps, confined at $B_z = 0.3$T. The peak output was ∼125MW, at ∼9.7GHz, corresponding to $\eta \sim 43\%$.

The prediction of peak efficiency at lower B-field is unusual, contrary to for example that seen in [31]. This may be understood in consideration of the previous discussion on the nature of the electron beam. If one begins by considering a nominally uniform density, annular, mono-energetic electron beam propagating close to the wall, the required external magnetic insulation to confine said beam is a function of both the electron energy and particle density. As the beam begins to undergo bunching via interaction with the EM-field, the local particle density begins to vary, as does the electron energy; for a given "bunch" the particle density has increased and the mean energy has reduced. This alters the interaction of the modulated e-beam with the applied B-field, meaning it impacts on the overlap of the local e-beam dimensions on the E_z field-profile. This influences the resonant frequency at which the SSCW couples to the eigenmode, and the strength of said coupling. This can be seen in the peak value of the frequency content of the output pulse, shown in Fig. 7 as a function of applied B_z over an extended range.

From this it can be seen that the best overlap, between the bulk of the bunched electron beam cross-section, and the EM-field pattern for the TM_{01} eigenmode at ∼9.7GHz, occurs at 0.3T, with higher B-field peak corresponding to operation at ∼9.6GHz. Essentially the spatial constraints on the extent of

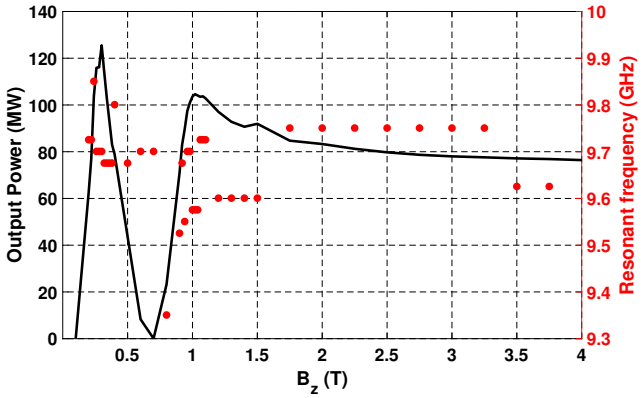

Fig. 7: The output power (solid) and peak resonant frequency (*), of the optimized BWO model over an extended range in B_z values, for fixed e-beam parameters of 210keV, 1.4kA, r_b = 15mm.

the bunched electron beam, at the higher B-field peak, appear such that the interaction with the EM-field pattern occurs most efficiently at a frequency slightly detuned from optimum, but still well within the operational "peak" one would associate with a source driven by a ∼4ns e-beam (see Fig. 9(b)). As the magnetic confinement is increased, the constraints on the bunched beam follow, with the result that, for $B_z > 3.5T$ the peak resonance settles at ∼9.2GHz, at ∼80MW (η ∼26%).

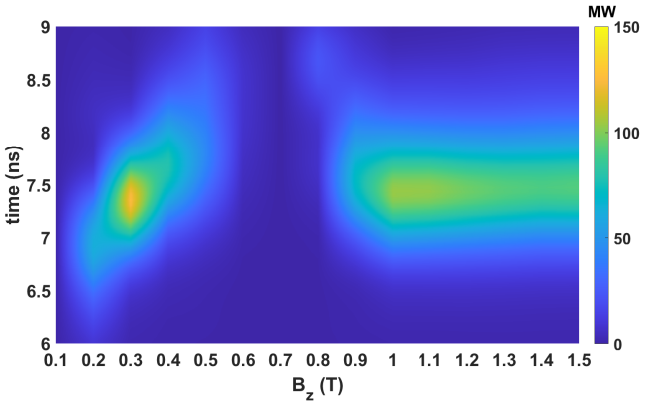

Fig. 8: Time evolution of the output power envelope, as a function of confining B-field, for the optimized BWO.

The impact of the magnitude of B_z, on the operation of the BWO, is also evident in the start-time of oscillations within the source. An inference that may be made from Fig. 6 and Fig. 7, is that the cases showing highest peak output powers correspond to instances where the oscillations started earliest, resulting in the most efficient modulation of the electron beam. This is borne out in Fig. 8, which shows the output power envelope of the BWO, as a function of time and applied B_z. From this it can be seen that the peak output at low B-field is not only higher, but also occurs earlier than the peak at high B-field (∼ 7.36ns and ∼ 7.45ns respectively). The variation is more pronounced at lower B-field, indicating a degree of control is required here when operating across

multiple sources, however it is not at a level that should prove problematic in experiment.

While the aim of the presented work was focused on optimizing the BWO using the maximum 4ns output from the RADAN 303B modulator, the impact of variation in e-beam duration, on operation of the BWO, was also considered. This indicated that while variation in the e-beam duration can affect both the temporal profile and peak output achieved, over the range of variation in e-beam duration expected in experiment ($\sim\pm$200ps) there was no negative effect. Extending the duration of the e-beam to the full 10ns runtime of the simulation the low B-field peak remained at 0.3T, achieving $\sim$110MW, with a slight shift in the temporal peak to $\sim$7.4ns. The high B-field peak shifted location to 1.5T, but remained less efficient, achieving $\sim$100MW at $\sim$7.7ns. Essentially the overall operation of the source remained unaffected. A more detailed study is required to fully characterize these effects over a suitably large range of e-beam durations, but this lies outwith the scope of the current work. The output power envelope and spectral content, for the optimized BWO model operating with a 4ns e-beam, are shown in Fig. 9(a)–(b) respectively.

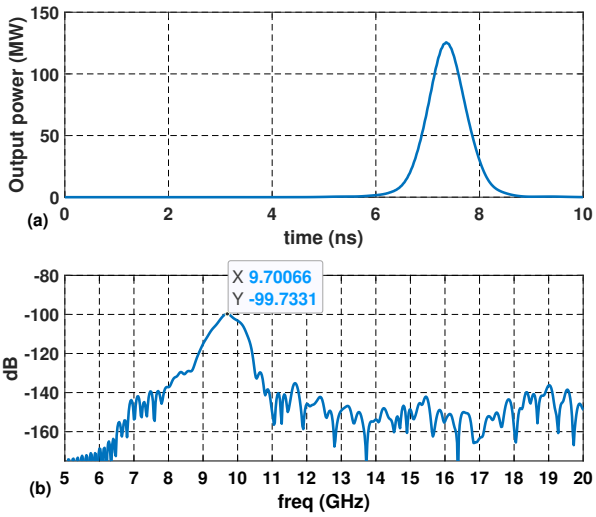

Fig. 9: The (a) power envelope and (b) spectral content, of the optimized BWO model.

IV. Analysis of the BWO in a Dual-Source Array

To phase-lock multiple like-sources, in the idealized case, would involve adjustment of the relative phase between identical output signals until they overlapped exactly in the far-field, producing an effective peak output power of N^2P_1, where P_1 is the peak output power from a single constituent source. In experiment it may be assumed some variation in the output signals will occur, due to differences in the individual assemblies and in the exact e-beam parameters. Taking the standard formula for calculating RMS power in an AC signal ($P_{rms} = V^2/2R$), the effective peak output power then follows

$$P_{eff} = \frac{(A_1 + A_2 + \dots A_N)^2}{2Z_0} \tag{8}$$

where A_N is the peak AC amplitude of the N^{th} source of the array and $Z_0 \approx 377\Omega$ is the impedance of free-space; noting that the port normalization employed in the PiC model effectively sets $Z_0 = 1\Omega$ for the results presented.

For a dual source array, driven by a single modulator, slight variations in the assemblies, between sources, will result in variations in the impulses applied to the individual diodes, most likely in terms of both their temporal phase and the impulse envelope. There will of course also be some slight variations in the assembly of the interaction regions, though high quality manufacture and careful assembly can minimize this. In addition, calibration of the electron accelerating diodes will be performed, to ensure the current drawn, for a given voltage, is consistent. In the following discussion, to allow for consideration of variation in experiment between sources, we will consider "like" operation to refer to both BWO's showing output of nominally 100MW, with a potential P_{eff} N^2 value of 400MW.

What remains is to evaluate the impact of variation in the e-beam rise-time (t_r) on individual source operation, and what that means for achieving phase-synchronization of the outputs across multiple sources.The effect of variation in t_r, over the range 50ps to 200ps, on BWO operation can be seen in Fig. 10. Both the magnitude, and temporal phase, of the peak in the output pulse are functions of t_r; this is quantified in Fig. 11, where the default value for t_r is taken as 100ps (inline with the rising edge of the applied impulse) and Δt refers to the detuning from this value.

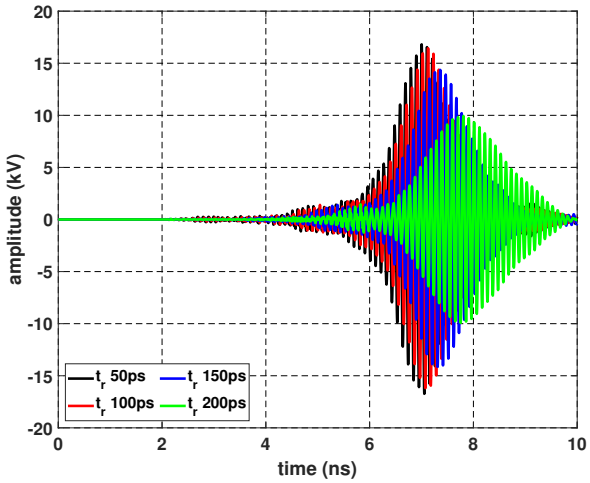

Fig. 10: Examples of the predicted output AC waveforms, from the optimized BWO, with t_r varied over the range 50ps to 200ps

From this it can be seen that HPM ($\geq$ 100MW) operation, from a single source, is predicted provided $t_r \leq$150ps. The peak output increases as t_r reduces, though the increase is less significant for $t_r \lesssim$ 100ps.

For effective far-field summation of the radiated field patterns this potential variation in t_r must be accounted for. To examine this, an analytic study was performed taking a fixed value of t_r for the first source ($t_{r1} = 100$ps), while t_{r2} (the

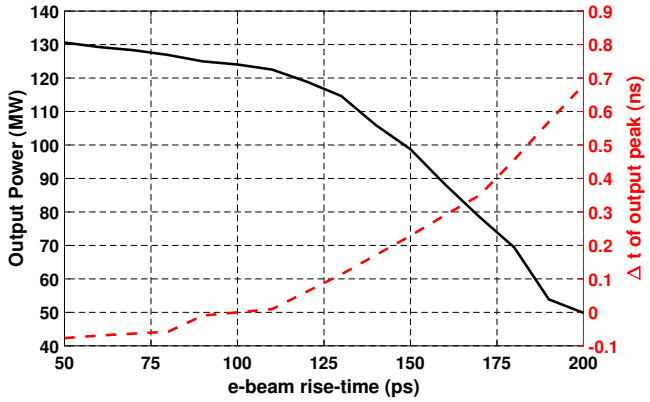

Fig. 11: Predicted peak output power (solid) from the optimized BWO, along with temporal phase of output peak (dashed), with t_r varied over the range 50ps to 200ps.

second source) was assumed to vary over the range 50ps to 200ps. Adjustment of the temporal phase (t_{ad}) of the second source's output was then considered over the range $t_{ad}\pm$300ps; this was taken as a proxy for temporal adjustment of the impulse signals driving the individual accelerating diodes. Using (8), the effective output power envelopes were then obtained, and their peak values (P_{eff}) recorded. The resulting surface map of the dependence of P_{eff} on t_{r2} and on t_{ad} is shown in Fig. 12.

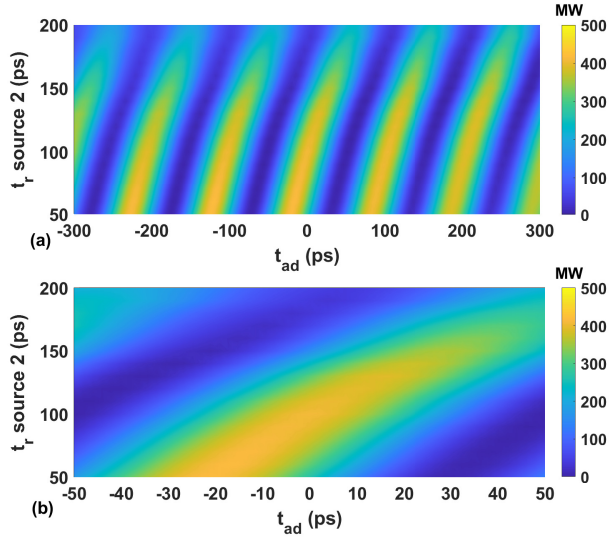

Fig. 12: Predicted P_{eff} for a dual-source array, with Source 2 t_r in the range 50ps to 200ps and (a) $t_{ad} = \pm$300ps, (b) $t_{ad} = \pm$50ps. Source 1 t_r was constant at 100ps.

Fig. 12(a) shows the periodic oscillation in peak-power one would expect, as the superimposed waveforms move in to and out of phase over the oscillatory period (τ ~100ps at ~9.7GHz) of the pulse. Further, while the absolute "peak" in output power travels as a discrete point in temporal phase, examination of Fig. 10 shows there are multiple oscillations comprising the effective "peak" of the output pulse. It is therefore possible to obtain P_{eff} in the region of N^2, at least where the peak-pulse duration is multiple integers of τ, without the need to fully account for the time delay between the absolute-peak outputs of the two sources. Indeed, from Fig. 12(b), it can be seen that P_{eff} >400MW may be maintained with timing adjustments on the order of $\pm$30ps, provided $t_{r2} \leq$ 150ps.

V. Conclusions

A numerical investigation of a relativistic BWO was undertaken, with the specific aim of obtaining HPM performance when driven by a short duration (4ns) e-beam at relatively low energy and beam current. Best performance was achieved using a 210keV, 1.4kA, thin annular e-beam, with $t_r = 100$ps and a 0.3T confining axial B-field, propagated through a 26-period long SWS of 13mm periodicity, with amplitude $\pm$1.6mm. This predicted a peak output power of ~125MW and an efficiency of $\eta \sim 43\%$. It was determined that $t_r \leq 150ps$ was required to maintain HPM operation, with the temporal phase of the output a relatively strong function of t_r.

An analytic study was performed to determine the impact of variation in t_r, across sources, in a dual-source array. Setting $t_{r1} = 100$ps, it was found that effective output powers, in the idealized N^2 range, could be obtained by adjusting the relative timing of the output pulses over the range $t_{ad} \pm 30$ps, provided $t_{r2} \leq 150$ps. This may be achieved in experiment via adjustment of the relative timing of the impulse signals, applied at the individual accelerating diodes; an attractive means of realizing this is presented in [33], which will be the subject of future work as the design of the BWO is progressed to experiment.

References

[1] J. H. Yang, Y. Zhang, J. Zhang, T. Shu, C. Li, "A new high power microwave source operated at low magnetic field", *Chin. Phys. Lett.*, vol. 20, no. 1, pp. 96–98, Jan. 2003, 10.1088/0256-307X/20/1/328.

[2] Z. Liu, H. Huang, X. Jin, L. Lei, "Design of an X-band gigawatt multibeam relativistic klystron amplifier", *IEEE Trans. Plasma Sci.*, vol. 42, no. 10, pp.3419–3422, 10.1109/TPS.2014.2354831.

[3] D. M. Goebel, E. A. Adler, E. S. Ponti, J. R. Feicht, R. L. Eisenhart, R. W. Lemek, "Efficiency enhancement in high power backward-wave oscillators", *IEEE Trans. Plasma Sci.*, vol. 27, no. 3, pp. 800–809, 10.1109/27.774686.

[4] R. Z. Xiao, X. W. Zhang, L. J. Zhang, X. Z. Li, L. G. Zhang, W. Song, Y. M. Hu, J. Sun, S. F. Huo, C. H. Chen, Q. Y. Zhang, G. Z. Liu, "Efficient generation of multi-gigawatt power by a klystron-like relativistic backward wave oscillator", *Laser and Particle Beams*, vol. 28, no. 3, pp 505–511, Sept. 2010, 10.1017/S0263034610000509.

[5] R. Xiao, C. Chen, W. Tan, Y. Teng, "Influences of the modulation cavity and extraction cavity on microwave generation and starting oscillation in a klystron-like relativistic backward wave oscillator", *IEEE Trans. Electron Devices*, vol. 61, no. 2, pp. 611–616, Jan. 2014, 10.1109/TED.2013.2295380.

[6] G. Wang, J. Wang, P. Zeng, D. Wang, S. Li, "Mode competition and selection in overmoded surface wave oscillator, *Phys. Plasmas*, vol 23, no. 5, article: 053113, May 2016, 10.1063/1.4951021.

[7] I. V. Konoplev, P. MacInnes, A. W. Cross, L. Fisher, A. D. R. Phelps, W. He, K. Ronald, C. G. Whyte, C. W. Robertson, "High-current electron beams for high-power free-electron masers based on two-dimensional periodic lattices", *IEEE Trans. Plasma Sci.*, vol. 30, no. 4, pp.751–763, April 2010, 10.1109/TPS.2009.2038161.

[8] Y. Teng, Y. Cao, Z. Song, H. Ye, Y. Shi, C. Chen, J. Sun, "A Ka-band TM02 mode relativistic backward wave oscillator with cascaded resonators", *Phys. Plasmas*, vol. 21, no. 12, article 123108, Dec. 2014, 10.1063/1.4902531.

[9] S. B. Harriet, D. B. McDermott, N. C. Luhmann Jr., "Experimental second-harmonic axis-encircling beam gyro-TWT amplifier", presented at the *32nd Int. conf. IRMMW*, Cardiff, UK, Sept. 2–9, 2007, 10.1109/ICIMW.2007.4516539.

[10] S. H. Gold, A. W. Fliflet, W. M. Manheimer, R. B. McCowan, W. M. black, R. C. Lee, V. L. Granatstein, A. K. Kinkead, D. L. Hardesty, M. Sucy, "High peak power Ka-band gyrotron oscillator experiment", *Phys. Fluids*, vol. 30, no. 7, pp. 2226–2238, July 1987, 10.1063/1.866157.

[11] M. R. Ulmaskulov, S. A. Shunailov, K. A. Sharypov, M. I. Yalandin, V. G. Shpak, S. N. Rukin, M. S. Pedos, "Four-channel generator of 8-GHz radiation based on gyromagnetic non-linear transmitting lines", *Rev. Sci. Instrum.*, vol. 90, no. 6, article: 064703, June 2019, 10.1063/1.5091075.

[12] N. S. Ginzburg, A. W. Cross, A. A. Golovanov, A. D. R. Phelps, I. V. Romanchenko, V. V. Rostov, K. A. Sharypov, V. G. Shpak, S. A. Shunailov, M. R. Ul'mascov, M. I. Yalandin, "Coherent summation of emission from relativistic Cherenkov sources as a way of production of extremely high-intensity microwave pulses", *IEEE Trans. Plasma Sci.*, vol. 44, no. 4, pp. 377–385, April 2016, 10.1109/TPS.2016.2517670.

[13] N. S. Ginzburg, A. W. Cross, A. A. Golovanov, G. A. Mesyats, M. S. Pedos, A. D. R. Phelps, I. V. Romanchenko, V. V. Rostov, S. N. Rukin, K. A. Sharypov, V. G. Shpak, S. A. Shunailov, M. R. Ulmaskulov, M. I. Yalandin, I. V. Zotova, "Generation of electromagnetic fields of extremely high intensity by coherent summation of Cherenkov superradiance pulses", *Phys. Rev. Lett.*, vol. 115, no. 11, article: 114802, Sept. 2015, 10.1103/PhysRevLett.115.114802.

[14] V. V. Rostov, A. A. Eichaninov, I. V. Romanchenko, M. I. Yalandin, "A coherent two-channel source of Cherenkov superradiance pulses", *Appl. Phys. Lett.*, vol. 100, no. 22, article: 224102, May 2012, 10.1063/1.4723845.

[15] K. A. Sharypov, *et al.*, "Coherent summation of Ka-band microwave beams produced by sub-gigawatt superradiance backward wave oscillators", *Appl. Phys. Lett.*, vol. 103, no. 13, article:134103, Sept. 2013, 10.1063/1.4823512.

[16] R. Xiao, Y. Deng, C. Chen, Y. Shi, J. Sun, "Generation of powerful microwave pulses by channel power summation of two X-band phase-locked relativistic backward wave oscillators", *Phys. Plasmas*, vol. 25, no. 3, article: 033109, March 2018, 10.1063/1.5022808.

[17] R. Xiao, Y. Deng, T. Shy, D. Yang, "Phase stabilization of a relativistic backward wave oscillator by controlling the cathode characteristics for a slowly rising voltage", *J. Appl. Phys.*, vol. 125, no. 17, article: 17330, May 2019, 10.1063/1.5093031.

[18] Y. Teng, *et al.*, "Phase locking of high power relativistic backward wave oscillator using priming effect", *J. Appl. Phys.*, vol. 111, no. 4, article: 043303, Feb. 2012, 10.1063/1.3686620.

[19] G. S. Nusinovich, O. V. Sinitsyn, J. Rogers, A. G. Shkvarunets, Y. Carmel, "Phase locking in backward-wave oscillators with strong end reflections", *Phys. Plasmas*, vol. 14, no. 5, article: 053109, May 2007, 10.1063/1.2734571.

[20] R. Xiao, Y. Wang, Y. Deng, X. Bai, Z. Song, "Particle-in-Cell demonstration of the effect of voltage rise time on phase synchronization in two parallel relativistic backward-wave oscillators", *IEEE. Trans. Electron Devices*, vol. 63, no. 3, pp. 1317–1321, Feb. 2016, 10.1109/TED.2016.2520500.

[21] G. A. Mesyats, S. D. Korovin, V. V. Rostov, V. G. Shpak, M. I. Yalandin, "The RADAN series of compact pulsed power generators and their applications", *Proc. IEEE*, vol. 92, no. 7, pp. 1166–1179, July 2004, 10.1109/JPROC.2004.829005.

[22] A. A. El'chaninov, A. I. Kilmov, O. B. Koval'chuk, G. A. Mesyats, I. V. Pegel, I. V. Romanchenko, V. V. Rostov, K. A. Sharypov, M. I. Yalandin, "Coherent summation of power nanosecond relativistic microwave oscillators", *Tech. Phys.*, vol. 56, no. 1, pp. 121–126, Feb. 2011, 10.1134/S1063784211010099.

[23] G. G. Denisov, M. G. Reznikov, "Corrugated cylindrical resonators for short-wavelength relativistic microwave oscillators," *Radiophys Quantum Electron*, vol. 25, pp. 407–413, May 1982, 10.1007/BF01035315.

[24] J. Benford, J. A. Swegle, E. Schamiloglu, *High Power Microwaves*, 3rd ed., pp 133–135, New york, NY, USA: Taylor & Francis, 2016, ISBN 9780367871000.

[25] J. A. Swegle, J. W. Poukey, G. T. Leifeste, "Backward wave oscillators with rippled wall resonators: analytic theory and numerical simulation", *Phys. Fluids*, vol. 28, no. 9, pp. 2882–2894, Sept. 1985, 10.1063/1.865209.

[26] B. N. Brejzman, D. D. Ryutov, "Powerful relativistic electron beams in a plasma and in a vacuum", *Nucl. Fusion*, vol.14, no. 6, pp. 873–907, Aug. 1974, 10.1088/0029-5515/14/6/012.

[27] S. Tamura, M. Yamakawa, Y. Takashima, K. Ogura, "Instability driven by a finitely thick annular beam in a dielectric-loaded cylidrical waveguide", *Plasma Fusion Res.*, vol. 3, article: S1020, Aug. 2008, 10.1585/prf.3.S1020.

[28] D. L. Fensternmacher, C. E. Seyler, "Nonlinear space-charge wave propagation on thin annular electron beams", *Phys. Fluids*, vol. 27, no. 7, pp. 1808–1814, July 1984, 10.1063/1.864793.

[29] A. I. Kilmov, I. K. Kurkan, S. D. Polevin, V. V. Rostov, E. M. Tot'meninov, "A multigigawatt X-band relativistic backward wave oscillator with a modulating resonant reflector", *Tech. phys. Lett.*, vol. 34, no. 3, pp. 235–237, March 2011, 10.1007/s11455-008-3017-z.

[30] S. Humphries, Jr., *Charged Particle Beams*, pg 450, available https://www.fieldp.com/cpb.html. Accessed on: Oct. 19 2021.

[31] N. S. Ginzburg, N. Yu. Novozhilova, I. V. Zotova, A. S. Sergeev, N. Yu. Peskov, A. D. R. Phelps, S. M. Wiggins, A. W. Cross, K. Ronald, W. He, V .G. Shpak, M. I. Yalandin, S. A. Shunailov, M. R. Ulmaskov, V. P. Tarakanov,"Generation of powerful subnanosecond microwave pulses by intense electron bunches moving in a periodic backward wave structure in the superradiative regime", *Phys. Rev. E*, vol. 60, no. 3, pp. 3297–3304, Sept. 1999, 10.1103/PhysRevE.60.3297.

[32] *CST: Studio Suite*, available https://www.cst.com. Accessed on: Oct. 15, 2021.

[33] M. R. Ulmaskulov, S. A. Shunailov, K. A. Sharypov, M. I. Yalandin, V. G. Shpak, "Modification of high-voltage pulse waveform by the spiral and core-transformer ferrite-filled lines", *IEEE Trans. Plasma Sci.*, vol. 45, no. 10, pp. 2707–2714, July 2017, 10.1109/TPS.2017.2727639.